PHYSICAL REVIEW B VOLUME 22, NUMBER 12 15 DECEMBER 1980

Bonding of fluorine in amorphous hydrogenated silicon

C. J. Fang,* L. Ley, H. R. Shanks,† K. J. Gruntz, and M. Cardona
Max-Planck-Institut für Festkörperforschung, Heisenbergstrasse 1, 7000 Stuttgart 80, Federal Republic of Germany
(Received 28 April 1980)

The infrared spectra of amorphous fluorinated silicon samples (*a*-Si:F,H) have been measured. The following lines were identified (in addition to the hydrogen-induced bands at 2090, 1985, 890, 840, and 630 cm^{-1}): 1010 cm^{-1} ($Si-F_4$ stretching); 930 cm^{-1} ($Si-F_2$, $Si-F_3$ stretching); 828 cm^{-1} (Si–F stretching); 510 cm^{-1} (Si TO mode induced by F); 380 cm^{-1} (SiF_4 bond bending); 300 cm^{-1} (Si–F, $Si-F_2$ wagging). The intensities of these bands were measured as a function of preparation condition and annealing temperature. In addition to the SiF_4 molecules trapped in the films during preparation, annealing temperatures above 300 °C produced a transformation of some Si—F groups into SiF_4 molecules. Gas-evolution experiments show that fluorine-containing molecules (F, HF, SiF_4) evolve all in one sharp peak around 680 °C, near the crystallization point. An average cross section $\bar{\Gamma}$ for Si–F vibrations of 11.2 cm^2/mmol and bond was obtained in good agreement with similar values in gaseous and solid SiF_4.

I. INTRODUCTION

The incorporation of hydrogen into amorphous silicon (*a*-Si:H) has led to a material that can be substitutionally doped similarly to crystalline silicon.[1] The doping efficiency, i.e., the change in conductivity for a given concentration of dopant atoms, is, however, much smaller than in crystalline silicon. This is due in part to a nonvanishing density of states in the energy gap of *a*-Si which is *reduced* through the addition of hydrogen to about 10^{17} states/eV cm^3 but not completely removed.

Recently, Madan *et al.*[2,3] have suggested that the addition of fluorine to *a*-Si:H (*a*-Si:H,F) results in a material with a doping efficiency higher than that of the merely hydrogenated substance. Furthermore, the room-temperature conductivity of their phosphorus-doped fluorinated material had a value of ~1 Ω^{-1} cm^{-1}, not previously obtained in amorphous hydrogenated silicon.

In the case of *a*-Si:H the investigation of the vibrational properties of the silicon-hydrogen bonds through infrared spectroscopy has provided considerable and detailed information on the bonding configurations of the hydrogen in the amorphous silicon network.[4-7] We have therefore carried out a similar investigation of *a*-Si:H,F. Their spectra were complemented by measurements of the hydrogen and fluorine concentrations using the nuclear reaction of the hydrogen with nitrogen (^{15}N, for the determination of the hydrogen content) and the electron microprobe technique, Auger and photoelectron spectroscopy, for the determination of the fluorine content. The thermal stability of hydrogen and fluorine was investigated in annealing and differential gas-evolution experiments.

II. THE PREPARATION OF FLUORINATED *a*-Si

Films of fluorinated *a*-Si were prepared by reactively sputtering a *c*-Si target in a gas mixture containing argon, hydrogen, and silicon tetrafluoride (SiF_4). A conventional rf sputtering system was used with a 5-cm diameter Si target opposite the substrate holder at a distance of 2 cm. The rf power applied to the Si target was typically 170 W. This corresponds to a specific power of 8.7 W/cm^2. The target was water-cooled whereas the substrates were allowed to attain a temperature of about 65 °C as determined by a thermocouple on the substrate holder during the sputtering process.

The base pressure of the sputtering vessel was 2×10^{-6} Torr obtained with a turbomolecular pump. After the initial pumpdown a flow of argon gas was adjusted so as to maintain a pressure of 10^{-2} Torr with the unthrottled pump. The flow rates of H_2 and SiF_4 were similarly adjusted to yield pressures in the range from 5×10^{-4} to 2×10^{-3} Torr. The deposition rate obtained with these parameters was approximately 1 μm/h. The samples investigated were between 1 and 2 μm thick.

Raman spectroscopy was used to check for possible crystallization in the films. At no time was the crystalline peak at 520 cm^{-1} observed in unannealed films.

III. RESULTS

A. Infrared spectra

The infrared transmission spectra were measured with a Perkin-Elmer double-beam spectrometer using a blank *c*-Si substrate as a reference. The infrared absorption coefficient $\alpha(\omega)$ was calculated from the transmission using the procedure

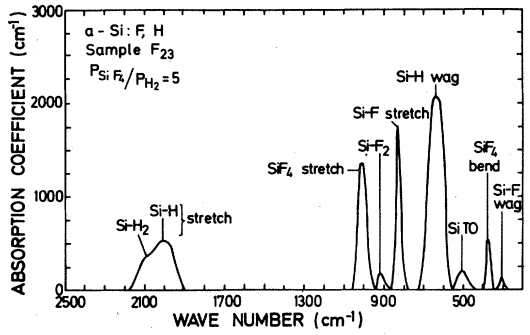

FIG. 1. The infrared spectrum of a-Si:F,H, prepared at room temperature.

of Brodsky *et al.*[4] Whenever intensities of absorption bands are given in what follows, they refer to the integrated absorption strength $I=\int[\alpha(\omega)/\omega]d\omega$ (in cm^{-1}).

From the interference fringes in the infrared spectra we deduced the refractive index n of our films. The average value obtained from ten samples prepared at room temperature is $\bar{n}=3.64 \pm 0.4$ at $\lambda=2.5$ μm. The standard deviation given reflects the accuracy of the measurements as well as systematic deviations in n depending on the amount of hydrogen and fluorine incorporated into the films. These results are consistent with previous determinations of n in a-Si:H.[5,6]

Figures 1 and 2 show the ir spectra of two films that differ in the relative contents of hydrogen and fluorine. Sample F_{23} was prepared with a ratio, r, of SiF_4 to H_2 partial pressures in the sputtering gas of 5 while sample F_{35} was deposited with $r=0.5$. As a consequence, F_{23} contains 10-at.% hydrogen and about 8-at.% fluorine, and F_{35} contains 15-at.% hydrogen and no more than 5-at.% fluorine. The hydrogen content of the films was determined by the nuclear reaction method and reevaluated in at.% using the atomic density of crystalline silicon (5×10^{22} cm^{-3}). The values

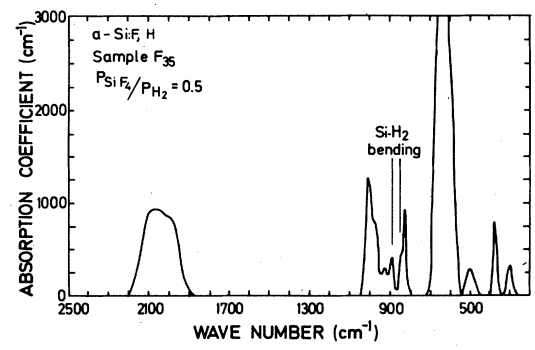

FIG. 2. The infrared spectrum of a-Si:F,H, prepared at room temperature.

quoted are accurate to within 10%. The fluorine concentrations were estimated from the strength of the fluorine-induced ir bands, a topic that will be discussed in Sec. IIID.

The Si–H stretching bands at 2090 and 1985 cm^{-1} and the wagging band at 630 cm^{-1} are readily identified in both spectra in analogy with the corresponding absorption peaks in hydrogenated a-Si (a-Si:H).[4,5] The frequencies are shifted downwards by 15 cm^{-1} (stretching) and 10 cm^{-1} (wagging) in the fluorinated samples. In the spectrum of sample F_{35} two weak structures at 840 and 890 cm^{-1} are ascribed to the Si–H_2 bending modes as they are observed in unfluorinated a-Si:H films with a predominant stretching band at 2100 cm^{-1}.

The remaining lines at 1010, 930, 828, 510, 380, and 300 cm^{-1} are fluorine-related vibrations. They are, as expected, stronger in F_{23} than in F_{35} which has only about half the fluorine content of F_{23}.

The bands at 1010 and at 380 cm^{-1} always occur together in our samples with a constant intensity ratio $I(1010)/I(380)=5.0\pm0.5$. We ascribe them to the bond-stretching (1010 cm^{-1}) and bond-bending (380 cm^{-1}) vibrations of SiF_4 molecules embedded in the a-Si matrix during the deposition process. The average Si–F bond-stretching frequency (longitudinal plus transverse) in solid SiF_4 is 1013 cm^{-1} and the average bond-bending frequency is 385 cm^{-1} according to the compilation of Bernstein and Meredith.[8] These values agree with the ones found in a-Si:F,H so closely that the assignment made seems quite reliable. Schatz *et al.*[9] have measured the cross sections of the two bands in crystalline SiF_4 and find $\Gamma(1013)/\Gamma(385)=5.2$ in perfect agreement with the corresponding intensity ratio measured in our films.

The Si–F stretching frequencies for a number of methyl- and fluorine-substituted silanes cover a range from 1013 cm^{-1} in SiF_4 to 858 cm^{-1} in $FSiH_2CH_3$.[10] These frequencies are influenced by the reduced mass of the vibrating system and by induction effects of the substituting groups which change the force constant of the Si–F bond. The latter is the dominant factor and it can be related to the electronegativity of the substituted groups in a phenomenological way.[10,11] Lucovsky[12] has elaborated on this approach for the Si–H bond, extending it to the case of the a-Si:H network. We have applied the procedure given by Lucovsky to the Si–F stretching frequencies. In Fig. 3 the Si–F stretch frequencies of a number of methylated and hydrogenated fluorosilanes are plotted versus the electronegativity of the substituted groups as defined by Sanderson.[13] The Si–F bond in a-Si:F corresponds to the arrow-marked F–$Si(Si)_3$ in Fig. 3.

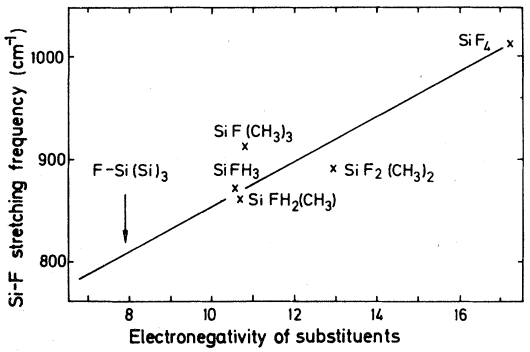

FIG. 3. The Si–F stretch frequencies of substituted fluorosilanes versus the electronegativity sum of the substituted radicals. The arrow marks the frequency expected for Si–F in a-Si:F,H.

In spite of the limited number of data points an approximately linear correlation between the electronegativities and the stretch frequencies can be inferred from Fig. 3. The frequency expected for the Si–F stretching vibration in a-Si:F is 810 cm^{-1}. The closest band in the spectra of Figs. 1 and 2 is that at 828 cm^{-1} which we ascribe consequently to that mode. This assignment agrees with that made earlier by Madan *et al.*[2,3] The frequency of the Si–F wagging mode can be estimated from the stretching frequency using the ratio of the bond-stretching to bond-bending force constants from SiF_4 (Ref. 9). This ratio is 8.2. We thus obtain a frequency of 291 cm^{-1} for the Si–F wagging mode in a-Si:F. The band closest to this value at 300 cm^{-1} in Figs. 1 and 2 is therefore identified with that mode.

The stretching modes for $Si-F_2$ and $Si-F_3$ configurations are expected to lie between those of SiF_4 and Si–F. The asymmetric line at 930 cm^{-1} is thus the most likely candidate for these modes. On the basis of statistics it should correspond mainly to $Si-F_2$.

Finally, the peak in the transmission spectra of Fig. 1 at 510 cm^{-1} lies within the TO band of the a-Si lattice [for c-Si TO(Γ) = 520 cm^{-1}, the peak in the density of TO states occurs at 490 cm^{-1}]. While this mode is ir inactive in the nonpolar Si network the addition of the highly electronegative F should induce enough charge transfer in its neighborhood to ir activate this mode in a-Si:F and shift it to 510 cm^{-1}. The fact that the intensity of this band scales with the Si–F and $Si-F_2$ vibrational modes but not with the SiF_4 modes supports this interpretation.

B. The annealing behavior of a-Si:F,H films

The hydrogen and fluorine content of the films as a function of annealing temperature, T_a, was monitored by gas-evolution experiments and by ir spectroscopy after a number of isochronal annealing steps. Samples were heated at a constant heating rate of 8 °C/min in a small UHV chamber. The evolving gases were allowed to escape through a 0.3-mm hole into another chamber of comparable volume equipped with a quadrupole mass spectrometer. This second chamber was pumped with a turbomolecular pump at a speed of 100 l/sec. Under these conditions (small pumping speed of the evolution chamber and high pumping speed of the detection chamber) the quadrupole signal is proportional to the *instantaneous* partial pressure of the corresponding species in the evolution chamber.[14] The quadrupole analyzer was programmed to scan repeatedly over preselected mass ranges during the annealing of the sample. In this way a quasicontinuous plot of the evolution rates of all gases of interest could be obtained in a single run.

The result of the gas-evolution measurement of sample F_{41} is shown in Fig. 4. Also shown for comparison are the evolution spectra of two samples containing no fluorine. One was prepared by sputtering Si in an $Ar-H_2$ mixture and the other was deposited by the glow discharge decomposition of SiH_4. All three samples were prepared at room temperature. Hydrogen evolves in two stages. In the samples containing no fluorine, evolution rates peak around 350 °C and around 550 °C. In the fluorinated sample the evolution maxima are shifted up to ~390 and 610 °C, respectively. Three fluorine-containing species could be identified in the mass spectra of all fluorine, evolution rates 19), HF (mass 20), and SiF_4 (mass 104). All three evolve in one narrow peak at 680 °C, just below the crystallization temperature of a-Si.

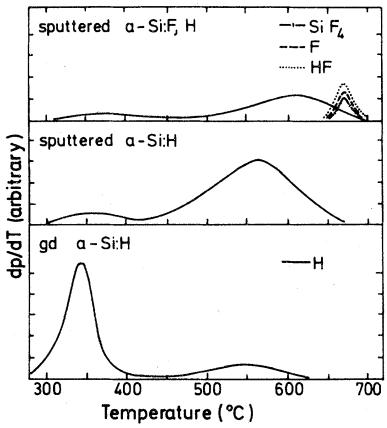

FIG. 4. Differential gas-evolution rates for three samples of a-Si:glow discharge a-Si(gd$a$-Si), sputtered a-Si and sputtered a-Si:H,F. The unmarked line represents the H evolution. The heating rate was 8 °C/min.

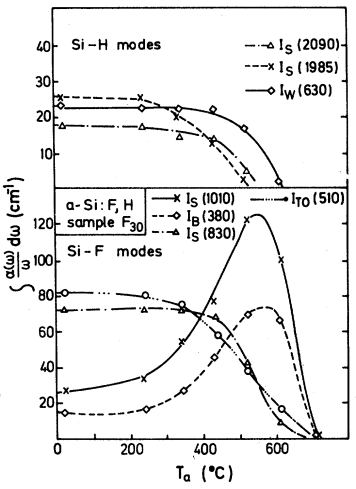

FIG. 5. Intensity of infrared modes as a function of isochronal annealing temperature for a-Si:F,H (sample F_{30}).

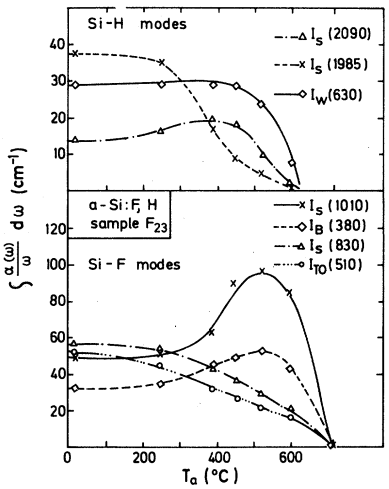

FIG. 6. Intensity of infrared modes as a function of isochronal annealing temperature for a-Si:F,H (sample F_{23}).

Small amounts of F_2 (mass 38) have been observed in some samples. Argon (mass 40 for Ar, equivalent mass 20 for Ar^+) usually evolves together with the hydrogen. The HF (mass 20) evolution rate in the spectrum of Fig. 4 has been corrected for the mass-20 contribution from Ar^+. The results of Fig. 4 are characteristic for all samples of a-Si:F,H studied.

Figures 5 and 6 depict the integrated absorption strengths of various ir bands after a series of isochronal annealing steps. It was necessary to keep the sample at least 20 min at each temperature. For shorter times, incomplete annealing was observed as witnessed by nonvanishing fluorine concentrations at the crystallization temperature of ~700 °C, due to a delayed evolution of fluorine-containing species.

The hydrogen bands show the annealing behavior observed earlier in nonfluorinated a-Si:H samples.[15] The wagging band at 630 cm^{-1} remains fairly constant initially and decreases rapidly above 400 °C when the majority of the hydrogen evolves (compare the gas-evolution data of Fig. 4). The 1985 and the 2090 cm^{-1} stretching modes behave differently in the two samples. In sample F_{30}, with approximately equal intensities of both bands, they follow essentially the wagging mode as a function of annealing temperature. Sample F_{23} has initially a 1985-cm^{-1} mode about 2.5 times as intense as the 2090-cm^{-1} mode. The two modes behave in a complementary way up to about 400 °C. This is in accord with a shift of the Si–H stretching frequency from 2000 to 2090 cm^{-1} with annealing temperature discussed in detail by Shanks *et al.*[15] It appears as a *decrease* in the strength of the 1985-cm^{-1} band and a corresponding *increase* in the 2090-cm^{-1} band. Above 400 °C both bands drop off together following the actual loss in hydrogen.

Four fluorine-related bands have been monitored as a function of T_a: the SiF_4 stretching and bending bands at 1010 and 380 cm^{-1}, the Si–F stretching band at 830 cm^{-1}, and the F-induced TO mode of the silicon network at 510 cm^{-1}. The latter two decrease monotonically with increasing annealing temperature at very much the same rate. The bands signalling the presence of SiF_4, however, increase (slowly initially, more rapidly above 300 to 350 °C) and peak around 530 °C. Beyond 600 °C they fall off rapidly and at 700 °C no fluorine-containing bands could be detected in the ir spectra. At this temperature the films have crystallized.

The refractive index of the films was also measured as a function of annealing temperature between 2.5 and 5 μm. It remains unchanged up to about 400 °C and increases by $(11 \pm 2)\%$ when the samples are annealed further up to 600 °C. This fact seems connected with the loss of hydrogen.

C. The hydrogen and fluorine content of a-Si:F,H as a function of preparation conditions

The amount of fluorine incorporated into the films and its bonding configuration (Si–F bonded to the amorphous network or free SiF_4 molecules) were monitored as a function of deposition parameters. The parameters varied were the rf power of the discharge and the ratio r of the SiF_4 to H_2 partial pressures. This ratio was varied by add-

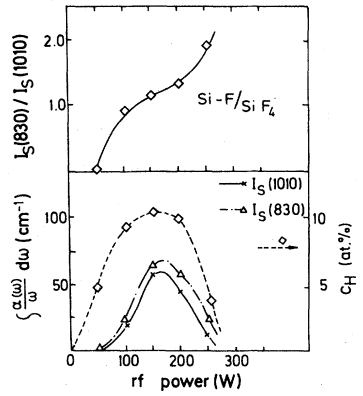

FIG. 7. Intensities of Si–F (830), SiF_4 (1010) bands, and the hydrogen concentration c_H as a function of rf power during sputter deposition.

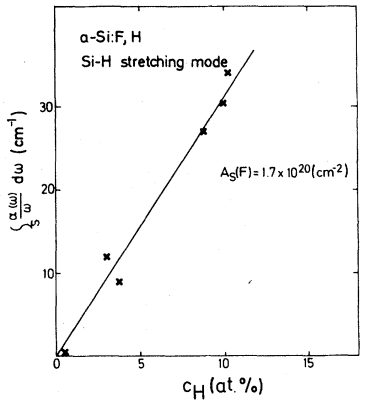

FIG. 9. Integrated strength of the Si–H stretching modes of a-Si:F,H samples (2090 and 1985 cm^{-1}) versus hydrogen concentration.

ing increasing amounts of SiF_4 to a constant pressure of H_2 and argon. The total pressure was thus changed by a factor of 2. Measurements were also performed for samples prepared without hydrogen ($r=\infty$ in the figures). In Fig. 7 the integrated strength of the absorption bands at 1010 cm^{-1} (SiF_4) and at 830 cm^{-1} (Si–F) are plotted versus rf power. The strength of both bands peaks at a power of ~160 W falling off to either side of this power. Below 50 W and above 300 W no fluorine could be incorporated into our films. It is also seen in Fig. 7 that the ratio of I_{830} to I_{1010} increases monotonically with increasing power. At low powers the fluorine is present almost exclusively in the form of SiF_4 trapped in the amorphous Si network, whereas at the highest power about twice as much fluorine is present bonded to the Si network than is in the form of SiF_4. This conclusion assumes comparable oscillator strengths per Si–F bond for both species.

The hydrogen concentration as determined by the nuclear-reaction technique is also plotted in Fig. 7. It is seen to follow essentially the intensity of the fluorine bands. The onset of measurable hydrogen concentrations is, however, shifted towards lower rf powers. At rf powers beyond ~300 W no deposition of a-Si:F,H could be observed.

The intensities of the Si–F and SiF_4 stretching bands as a function of the SiF_4 to H_2 mixing ratio r are plotted in Fig. 8 together with the hydrogen concentration. The hydrogen concentration is constant at 7.5 at.% as may be expected for a constant hydrogen partial pressure. For $r=\infty$, i.e., $p_{H_2}=0$, c_H drops of course to zero. The intensities of both fluorine bands increase initially as the fraction of SiF_4 to the gas mixture increases and also as the total pressure increases. The Si-F configuration is, however, clearly favored over SiF_4 for gas mixtures "lean" in H_2, and also at high pressures.

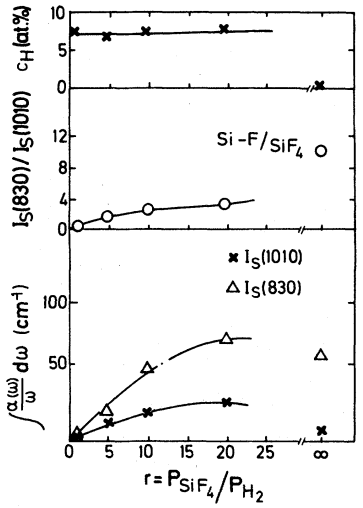

FIG. 8. Same as Fig. 7 as a function of the partial SiF_4 pressure for constant-H_2 pressure in the sputter gas.

D. The absolute fluorine and hydrogen concentration in a-Si:F,H

The hydrogen concentration of the samples was measured using the $^{15}(N,p)$ reaction.[16] This gives the absolute hydrogen content of the films which has been recalculated in terms of a relative hydrogen concentration c_H using the atomic density of crystalline silicon (5×10^{22} cm^{-3}). The integrated strength of the two Si–H stretching bands (I_s) and that of the Si–H wagging band (I_w) are plotted versus c_H in Figs. 9 and 10. The relationship between

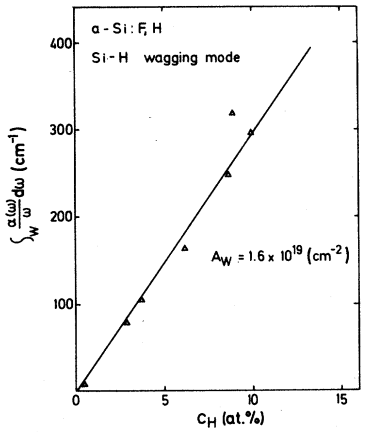

FIG. 10. Integrated strength of the Si–H wagging mode of a-Si:F,H samples (640 cm^{-1}) versus hydrogen concentration.

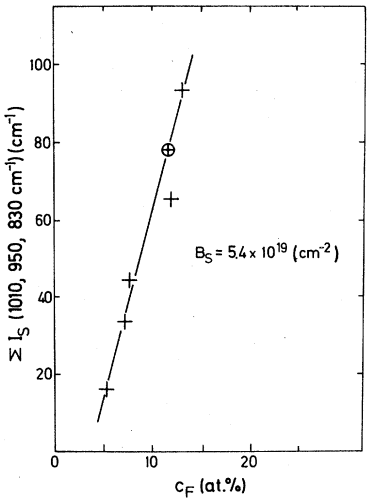

FIG. 11. Integrated strength of all Si–F stretching bands (Si–F, Si–F_2, SiF_4) versus fluorine concentration. The circle marks the value where the XPS and microprobe measurements of C_F were matched.

I_s, I_w, and c_H can be approximated by a straight line which gives proportionality constants $A_s(F)$ and $A_w(F)$ according to

$$N_H = A_{s,w}(F) I_{s,w},$$

where N_H = number of hydrogen atoms/cm^3. The numerical values so obtained are, expressed in units of atoms/cm^2,

$$A_s(F) = 1.7 \times 10^{20}$$

and

$$A_w(F) = 1.6 \times 10^{19}.$$

The value for $A_w(F)$ agrees with the corresponding one $[A_w(H)]$ for unfluorinated a-Si : H samples obtained earlier.[15] $A_s(F)$ is slightly larger than the average value of $A_s(H)$ (1.4×10^{20}), a fact which is not unexpected in view of the sensitivity of the stretching bands to local field corrections discussed in detail elsewhere.[15]

The fluorine content of our samples was determined in three different ways: by microprobe analysis, Auger-electron spectroscopy, and in one case by means of x-ray-induced photoelectron spectroscopy (XPS). Owing to difficulties in calibrating the microprobe with nonconducting fluorine-containing compounds we used the results of the microprobe analysis only as a relative measure of the fluorine content of our samples. These relative concentrations were put on an absolute scale by measuring the relative amounts of fluorine and silicon in one of the samples with XPS. The intensities of the Si 2p and F 1s core levels were used in conjunction with the appropriate cross sections from Ref. 17. In Fig. 11 we have plotted the fluorine concentrations so obtained versus the sum of the integrated absorption strength of all Si–F stretching bands at 1010 cm^{-1} (SiF_4), 930 cm^{-1} (Si-F_2), and 830 cm^{-1} (Si–F). For fluorine concentrations above 5 at.% the points can be connected by a straight line, i.e., the sum of the integrated absorption strength of the ir bands is proportional to the fluorine content. The proportionality constant B_s is defined through $N_F = B_s \sum I_s + 1.8 \times 10^{21}$, where N_F is the number of fluorine atoms and 1.8×10^{21} cm^{-3} reflects the nonzero intercept. B_s has the numerical value $B_s = 5.4 \times 10^{19}$ cm^{-2}. This value corresponds to an *average* effective cross section $\bar{\Gamma}'_{Si-F} = 11.2$ cm^2/mmol. This cross section is referred to one mmol of Si–F *bonds* and contains implicitly the effects of local-field corrections to the ir absorption strength of the Si–F modes.

Depth profiles of the fluorine content of some films were measured using Auger spectra while removing the sample surface continuously through high-energy argon-ion bombardment. In this way constant fluorine concentration between 1 and 3 at.% for all samples was obtained. The accuracy estimated for absolute concentrations in these measurements is approximately a factor of 2. These values are nevertheless considerably lower than measured by microprobe and XPS.

IV. DISCUSSION

A. The incorporation of SiF_4

The presence of SiF_4 molecules in amorphous fluorinated Si is one of the main findings of the present investigation. We must assume that the rather large SiF_4 molecule is trapped in the a-Si

network. Whether this trapping occurs inside of voids which can accommodate a number of molecules or at isolated sites cannot be decided on the basis of our data. A similar incorporation of SiH_4 molecules into a-Si:H has not been reported. The bigger size of the SiF_4 molecule with a bond length of 1.54 Å compared to the 1.45 Å for SiH_4 (Ref. 18) may, in part, be responsible for this fact. The considerably higher stability of the SiF_4 molecule with a dissociation energy of 589.7 kcal/mol compared to the 319.5 kcal/mol (Ref. 18) of the SiH_4 molecule is considered the key factor determining the presence of SiF_4. This view is supported by the results of Fig. 7. The likelihood of SiF_4 incorporation *decreases* relative to the Si–F formation with increasing power put into the plasma and therefore with increasing temperature of the rf plasma.

The results of Fig. 8 can be understood in terms of two competing processes: the formation of Si–F and Si–H in the plasma while the concentration of SiF_4 remains constant over a wide range of the mixing ratio r. We have to assume that the sputtering rate of Si is constant (the argon pressure remains the same throughout) and that H and F ions compete for the free bonds that are exposed during the deposition of a-Si. Since the hydrogen pressure remains constant the number of H atoms incorporated stays the same (except for the point at $r=\infty$, i.e., $p_{H_2}=0$). The fluorine concentration increases with r as the number of F ions available increases while the ratio of Si–F to SiF_4 grows slightly with r. For $r=\infty$, the sites that were taken up by hydrogen are now available for the attachment of F and the ratio SiF to SiF_4 increases. It should be noted that this increase in Si–F to SiF_4 takes place simultaneously with a decrease in the total amount of F incorporated for $r=\infty$.

The annealing experiments of Figs. 5 and 6 indicate a growth of the SiF_4-induced bands at the expense of the Si–F-induced bands above ~300 °C. Since the gas-evolution data (Fig. 4) indicate no loss of fluorine below 670 °C these data imply a transformation of Si–F or $Si–F_2$ configurations to SiF_4 molecules. This conclusion is supported by considering the two spectra of Figs. 12 and 13. The sample of Fig. 12 corresponds to the case already discussed. An initially intense band at 830 cm^{-1} due to Si–F bonds decreases at 610 °C while the band at 1010 cm^{-1} (SiF_4) increases by about the same factor. The sample of Fig. 13 was prepared with a Ge target and in this way the 1010-cm^{-1} band is dominant and only a minute number of Si–F bonds is present. When this sample is annealed no increase in the SiF_4 band is observed because there was too little Si–F present to contribute to it via the transformation described

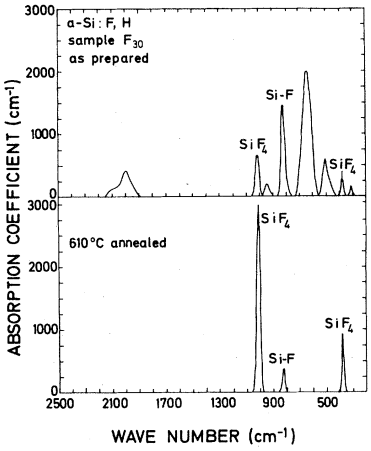

FIG. 12. ir spectra of a-Si:F,H before and after annealing at 610 °C, sample F_{30}.

above. The reaction path that leads to this transformation is not clear at present. It seems unlikely, however, that it involves exchange reactions with Si–H containing radicals. The probability of finding F–Si–H groups is too small at the H and F concentrations found in these samples. The evolution of SiF_4 species in addition to F and HF at 680 °C indicates that the transformation of Si–F into SiF_4 is not complete.

The presence of SiF_4 molecules is also, at least partially, responsible for the difference in F content measured by microprobe analysis and XPS on one side and by Auger spectroscopy on the other. The removal of surface layers through sputtering during the Auger analysis frees trapped SiF_4 molecules. They thus escape detection in the Auger spectrum. SiF_4 molecules in subsurface layers are not detected due to the low sampling depth (a few angstroms) of Auger spectroscopy.

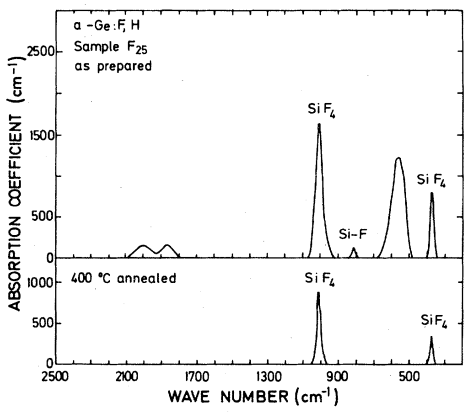

FIG. 13. ir spectra of a-Ge_xSi_{1-x}:F,H before and after annealing at 400 °C, sample F_{25}.

From the differences in fluorine concentration as measured by the two techniques we expect 30% to 50% of the fluorine to be present in the form of SiF_4 in our films.

This SiF_4 concentration is in accord with the absorption strength of the corresponding ir modes, provided the oscillator strength per Si–F is the same in all configurations. The changes in the 1010-cm^{-1} and 828-cm^{-1} band upon annealing (Figs. 5 and 6) suggest that this is indeed the case.

B. Intensity of the fluorine-induced ir bands

From the linear relationship between the fluorine concentration and the integrated strength of all fluorine involving stretching bands in Fig. 11 we deduced an average cross section for these vibrations of $\bar{\Gamma}'_{Si-F} = 11.2$ cm^2/mmol of Si–F bonds. The prime indicates that this value includes the enhancement of Γ due to local field contributions to the external field.

Schatz and Hornig[9] have measured the absolute intensity of the stretching band in gaseous SiF_4. They obtain a value of $\Gamma_{gas} = 58.3/4 = 14.6$ cm^2/mmol per Si–F bond. The local-field and refractive-index corrections are, in the simplest possible approximation[4]:

$$\Gamma_{gas} = \frac{(1+2\epsilon_m)^2\sqrt{\epsilon_m}}{9\epsilon_m^2}\,\Gamma_{solid}, \tag{1}$$

where $\epsilon_m \simeq 12$ is the long-wavelength electronic dielectric constant of a-Si. Equation (1) yields

$$\Gamma_{gas} \simeq 1.6\Gamma_{solid} = 18 \tag{2}$$

expressed in units of cm^2/mmol. This cross section Γ_{gas} is somewhat larger than that measured by Hornig but the discrepancy should not be taken too literally in view of the uncertainties involved in local-field corrections.

The cross section for Si–F bands can also be calculated from the LO-TO splitting observed in solid SiF_4 using the Lyddane-Sachs-Teller relation. We obtain for the absorption cross section per bond, including a Clausius-Mossotti type of local-field correction, valid for *homogeneous* solid SiF_4 (Ref. 19)

$$\Gamma_{gas} = \left(\frac{3n}{n^2+2}\right)^2 \frac{2\pi^2(\omega_{LO}-\omega_{TO})}{4V}, \tag{3}$$

where ω_{LO} and ω_{TO} are the longitudinal and transversal optical phonon frequencies, respectively. The refractive index n of SiF_4 is extrapolated from the values for $SiBr_4$ (1.56) and $SiCl_4$ (1.41) to be 1.26 (Ref. 20). V, the specific volume, is 20.4 cm^3/mmol. For the LO-TO splitting we take the value of 67 cm^{-1} measured by Bernstein and Meredith[8] for the bond-stretching modes. With these numerical values we obtain, again in cm^2/mmol,

$$\Gamma_{gas}(\text{bond stretching}) = 18. \tag{4}$$

This result agrees quite well with that of Eq. (2) and is also higher than that found by Schatz-Hornig.[9] We should point out, however, that the agreement between Eqs. (4) and (2) may be somewhat fortuitous as the LO-TO splittings reported in Ref. 19 may be somewhat enhanced by crystal-field effects (Davidov splittings).[21] Hence the result of Eq. (4) is to be regarded as an upper limit compatible with the observed splittings.

After submission of this manuscipt, Shimada, Katayama, and Horigome reported infrared-spectra measurements on similar films.[22] However, they assigned the absorption peaks at 1010 and 828 cm^{-1} to SiF_3 asymmetric and symmetric stretching modes, respectively. This assignment requires that the ratio of the intensities of the 1010- to 828-cm^{-1} bands be 2 to 1, or less if a Si-F stretching band is also contributing near 828 cm^{-1}. On a number of occasions we obtained films with ratios considerably greater than 2 in direct disagreement with this assignment.

ACKNOWLEDGMENTS

We are indebted to S. Kalbitzer for providing us with the results of the nuclear reaction measurements, to J. Stuke for the samples glow discharge (gd) a-Si:H, to A. J. Bevolo for his help with the Auger measurements, and to A. Breitschwerdt for the ir measurements. The technical help of W. Neu, G. Krutina, and R. Gibis is greatly appreciated.

---

*On leave from Chinese University of Science and Technology, Beijing, People's Republic of China.

†On leave from Ames Laboratory, USDOE, Ames, Iowa.

[1]W. E. Spear and P. G. Le Comber, Solid State Commun. 17, 1193 (1975).

[2]A. Madan, S. R. Ovshinsky, and E. Benn, Philos. Mag. B 40, 259 (1979).

[3]A. Madan and S. R. Ovshinsky, J. Non-Cryst. Solids 35–36, 171 (1980).

[4]M. H. Brodsky, M. Cardona, and J. J. Cuomo, Phys. Rev. B 16, 3556 (1977).

[5]C. C. Tsai and H. Fritzsche, Sol. Energy Mater. 1, 29 (1979).

[6]E. C. Freeman and W. Paul, Phys. Rev. B 20, 716 (1979).

[7]G. Lucovsky, R. J. Nemanich, and J. C. Knights, Phys. Rev. B 19, 2064 (1979).

[8]E. R. Bernstein and G. R. Meredith, J. Chem. Phys. 67, 4132 (1977).
[9]P. N. Schatz and D. F. Hornig, J. Chem. Phys. 21, 1516 (1953).
[10]H. Kriegsman, Z. Anorg. Allg. Chem. 294, 113 (1958).
[11]A. L. Smith, N. C. Angelotti, Spectrochim. Acta, 1959, 412; E. A. v. Ebsworth, M. Onyszchuk, and N. Sheppard, J. Chem. Soc. 1958, 1453.
[12]G. Lucovsky, Solid State Commun. 29, 571 (1979).
[13]R. T. Sanderson, Chemical Periodicity (Reinhold, New York, 1960), pp. 15–56.
[14]J. B. Condon, R. A. Strehlow, and G. L. Powell, Anal. Chem. 43, 1448 (1971).
[15]H. Shanks, C. J. Fang, L. Ley, M. Cardona, F. J. Demond, and S. Kalbitzer, Phys. Status Solidi B 100, 43 (1980).
[16]M. H. Brodsky, M. A. Frisch, and J. F. Ziegler, Appl. Phys. Lett. 30, 561 (1977).
[17]R. C. G. Leckey, Phys. Rev. A 13, 1043 (1976).
[18]Gmelin Handbuch der Anorganischen Chemie, Silizium Teil B (Verlag Chemie, Weinheim, 1959), pp. 234–237, 619–621.
[19]F. Besette, A. Cabane, R. P. Fournier, and R. Savoie, Can. J. Chem. 48, 410 (1970).
[20]Landolt-Börnstein: Numerical Data and Functional Relationships in Science and Technology, Series (Springer, Berlin, 1962), Teil 8, pp. 5–564.
[21]V. Schettino, Chem. Phys. Lett. 18, 535 (1973).
[22]T. Shimada, Y. Katayama, and S. Horigome, Jpn. J. Appl. Phys. 19, L265 (1980).